Journal of Applied Mechanics Vol.8, pp.943-948 (August 2005) JSCE

Structural identification using static macro-strain measurements from long-gage fiber optic sensors

Suzhen Li*, Zhishen Wu**

* Dr. Candidate of Eng., Dept. of Urban & Civil Eng., Ibaraki University, Hitachi, Ibaraki 316-8511
** Dr. of Eng., Prof., Dept. of Urban & Civil Eng., Ibaraki University, Hitachi, Ibaraki 316-8511

For global monitoring of large-scale civil infrastructures, it requires direct and accurate macro-deformation measurements to characterize the different performances of entire structural element. The conventional "point" static strain measurements are difficult to provide sufficient information for structural damage identification due to their localized behavior. In this regard, a novel packaging method for practical adaptation of long-gage FBG strain sensors in large-scale structures is proposed. Some static tests are carried out to verify the ability of the proposed FBG sensor for macro-strain measurements by comparing with that of foil strain gauge. Combined with a parametric identification method based on static macro-stain measurements, the applicability of the distributed long-gage FBG sensors in structural parameter estimation and damage detection is discussed. An experimental study of a beam specimen shows the advantage of the proposed sensor for structural identification over traditional strain gauge.

Key Words: macro-strain, distributed, long-gage, FBG sensors, structural identification

1. Introduction

As a novel and advanced sensing technique, optical fiber sensor has extended its potential advantages for structural health monitoring and damage detection. FBG sensor, which performs as a promising fiber optic sensor, has been developed for various purposes of measurements such as strain, temperature, acceleration, inclination, crack and so on. Although many researches have drawn attention to the practical application of FBG sensor in civil structures and some projects have brought it from laboratory to field, most of them focused on the usage of FBG sensor as a localized gauge for point or axial strain measurements, as applied in bridge cables and piles [1-3]. To catch structural information related to structural global characters rather than to local material behaviors, recently long-gage deformation sensor has attached some researchers' interest due to its ability to measure macro-deformations and flexibility for topologies and networks [4-6].

Compared with extensive structural identification techniques based on the dynamic measurements, limited work has been done by direct use of static test data, especially the static macro-strain measurements. Banan et al.[7-8] proposed two output error estimators to identify member constitutive properties based on a FE model and made a simulation study on a truss bridge structure. The problem on incomplete measurements was discussed as well. Sanayei et al. [9-11] presented a structural parameter identification method utilizing elemental strain measurements and mentioned that once static strains can be measured with a high precision, there are sufficient advantages to merit their use in many situations particularly for large structures whose displacements would require considerable labor to measure. Meanwhile, the influence of measurement noise on parameter estimation was studied in a statistical way and the relationship between the input and output errors was established based on error sensitivity analysis. Hjelmstad and shin [12] have also done some extensive work on structural damage detection using static response. They propose an adaptive parameter group subdivision algorithm to localize damage when the measured data are sparse and use a data perturbation method to establish the damage threshold above which damage can be confidently discerned from noise. Yeo et al. [13] introduced a regulation technique to alleviate the ill-posed ness of the system identification problem.

In this study, a novel packaging method for practical adaptation of long-gage FBG strain sensor is first proposed. Static tests are carried out to testify the effectiveness of the packaged long-gage FBG sensors for macro-strain measurements. Based on the previous work of Sanayei et al. [9-11] and Hjelmstad and shin [12], a static macro-strain based parametric identification method is presented, which is verified by using measurements from the proposed distributed

long-gage FBG sensors.

2. Packaged long-gage fiber Bragg grating strain sensor

2.1. Long-gage FBG strain sensor

In addition to the advantages of fiber optic sensors including electromagnetic noise immunity, electrically passive operation, low weight penalty, high sensitivity and easy multiplexing capability, the FBG strain sensors show some potential merits over other fiber optic sensors for structural parameter and damage identification, which can be stated as the following four respects. (1) Through special packaging (see 2.2) to extend original Bragg grating with inherent gage lengths on the order of a few millimeters to effective gauge length up to several centimeters or meters, FBG sensor can measure average macro-strain that is less susceptible to local stress/strain concentrations and hence more representative of the deformation of the entire structural member, which brings significant benefits for the global monitoring of structures. (2) Compared with resistive foil strain gauge and other traditional "point" gauges, FBG sensor can be easily multiplexed at many locations (currently, up to 64 FBGs can be theoretically wavelength-multiplexed in one fiber cable) and permit distributed strain measurements with high precision, which helps to obtain relatively complete information to solve the problem of instability including non-uniqueness and discontinuity of solutions that many identification algorithms have encountered. (3) Compared with linear variable displacement transducers (LVDT's), FBG sensor can identify accurate and exact modal macro-strain vectors, which in a sense are equivalent to curvature mode shape and have a clear relationship with rotational degree. Thus, FBG sensors possess a potential to bridge a gap of the application of static identification method to laboratory tests and practical engineering which is troubled with the well-known difficulty for effective and efficient displacement measurements.

2.2. Packaging design of long-gage FBG sensors

Despite a lot of potentials of FBG sensors for structural health monitoring as many researchers reported, their practical applications to civil engineering structures still face some primary technological challenges such as the problems of installation, durability, stability and reliability due to the fragility of bare fiber whose coat has to be removed from commercial optical fiber to fabricate FBG with high sensitivity. Moreover, appropriate methods for FBG sensor packaging and bonding with host structures should be carefully considered to protect the brittle fiber from harsh environment and ensure measurements of interest to transfer fully from object structure to sensors. In addition, the traditional problem that exists in most of fiber optic sensors of cross-sensitivity between strain and temperature needs to be resolved as well. Furthermore, uniform mechanical behavior along the sensing area is necessary to obtain the average macro-strains of structures and prevent the split of reflected Bragg wavelength peak and broadening of reflected spectrum band width.

Regarding the issues mentioned above, a novel packaging method for practical adaptation of long-gage FBG strain sensors for civil structural health monitoring is proposed, as shown in Fig.1. The detailed considerations can be expressed as follows:

(1) Special epoxy resin is used for recoating bare fiber including FBG because (a) the bare fiber is vulnerable to be strained directly and needs to be strengthened; (b) many researches have shown that no sliding appears and hence the strain compatibility can be achieved between the coat-removed glass fiber and epoxy resin at loads lower than the breaking strength of the fiber [14]; (c) the sensitivity of FBG to temperature can be adjusted by bonding with different kinds of epoxy materials, which makes it possible to limit the influence of temperature on FBG sensor within the permission of practical civil engineering [15]. Notice that the uniform bonding between glass fiber and recoated materials is very important for the sake of maintain same mechanical behavior.

(2) The hollow tube of gauge length inside the proposed device for sleeving the recoated FBG is essential to ensure that every point within the sensing area to be strained identically and hence the strain transferred from the shift of Bragg center wavelength can represent the average strain along the gauge length. The recoated FBG should be pre-tensioned enough to obtain accurate strain measurements under compression.

(3) Composite materials are chosen to connect the recoated bare fiber including FBG which works as a sensing part and common single-mode optical fiber cable (SMC) for (a) composite materials in the state of small strain show excellent mechanical bonding with other civil structural materials such as concrete, steel and FRP profiles; (b) the radial rigidity of composite materials can prevent the FBG from damage caused by lateral pressure; (c) the coefficient of thermal expansion (CTE) of composite materials is designable due to its dependence on type and volume ratio of fiber and resin [16], to make the sensor and host structure possess the same CTE and work well together [l]; (d) extensive researches have shown numerous advantages of composite materials for engineering practice such as durability, endurance to extreme environments including heat and corrosion and long-term stability.

(4) By connection with SMC, the proposed sensor can follow the common guide regulations for cable installation and connector protection. Moreover, small size (of 1mm diameter) and light weight make it easy to be either embedded in or surface adhered on the target structure.

(5) Multi-point or distributed measurements can be carried out easily by packaging an array of FBGs written in a single optical fiber or combining a set of individual packaged sensors using connectors.

2.3. Manufacture of long-gage FBG sensors

Based on the above-mentioned conceptual design but limited by current technological condition in the lab, the sensor is fabricated in a simple way as processed by the following steps (see Fig.2): (1) bare optical fiber of certain length including FBG without recoating with epoxy resin is used directly as the sensing part, which can work as well as the proposed sensor in the case of laboratory tests except the problem of temperature compensation which can be solved by using a dummy reference Bragg grating subjected to the same thermal environment but free from load; (2) instead of the hollow composite device for sleeving FBG, a plastic tube is sandwiched between two layers of carbon fiber tow and packaged together with optical fiber by epoxy resin; (3) FBG should be pre-tensioned before packaging for compressive measure.

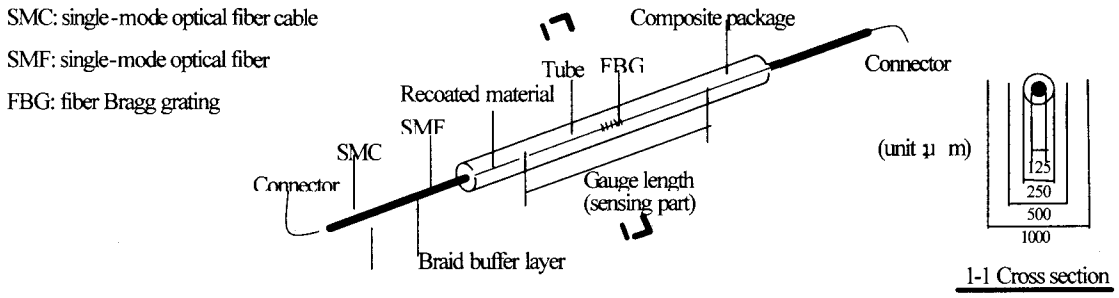

Fig. 1 Packaged long-gage FBG strain sensor

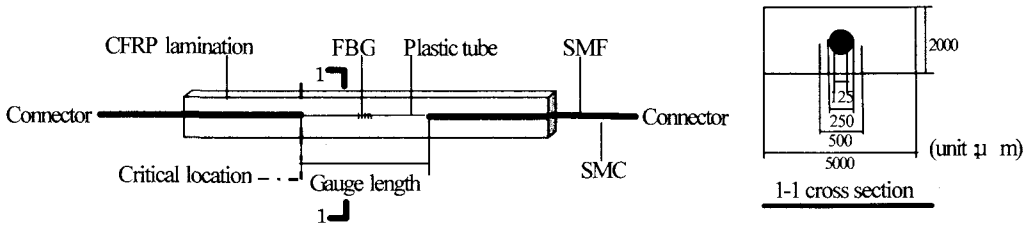

Fig.2 Embedded long-gage FBG sensor in CFRP lamination

Table 1 Static strains of intact steel specimen under uniaxial tension

load(KN)		0	10	20	30	40	50	80	100	120	150	180	200
strain gauge	Strain(με)	0	98	201	299	398	500	808	1004	1209	1513	1812	2016
bare FBG	Strain(με)	0	100	204	305	403	498	791	985	1176	1465	1758	1941
	Error* (%)	-	2.3	1.7	2.1	1.3	0.4	2.1	1.9	2.7	3.1	3.0	3.7
packaged FBG	Strain(με)	0	94	194	284	381	479	776	959	1156	1453	1741	1931
	Error* (%)	-	3.8	3.2	4.9	4.2	4.2	4.0	4.5	4.4	3.9	3.9	4.2

* Relative error of strains from FBG sensor to those from strain gauge

Single-mode optical fiber of Corning SMF-28 was utilized in this study. All the FBGs available for commerce passed 100KPSI proof test and basically could be used to measure strains up to 5000$\mu\varepsilon$ repeatedly. But during the process for packaging in the lab, the fiber had to suffer from coat-removing by mechanical stripper and fusion, which weakened the mechanical property of fiber and limited the measured upper bound down to about 2500$\mu\varepsilon$. Meanwhile, an FBG-Interrogation system from NTT-AT with sampling rate of 50Hz was used for data acquisition and signal interpretation.

3. Static tests of the proposed FBG sensors

3.1. Steel specimen under uniaxial tension

The static strains of an intact steel specimen with rectangular section of 50mm×10mm under uniaxial tension obtained by strain gauges, bare FBG fixed at two points and packaged FBG sensors of 10cm gauge length bonded at full length are summarized in Table 1. The relative errors of strains from different gauges show that FBG sensors can obtain static strains accurately and the proposed packaging method has little influence on measurements.

To verify the effectiveness of packaged long-gage FBG sensors for macro-strain measurements under uniaxial tension, as shown in Fig3(a), a steel board with rectangular section of

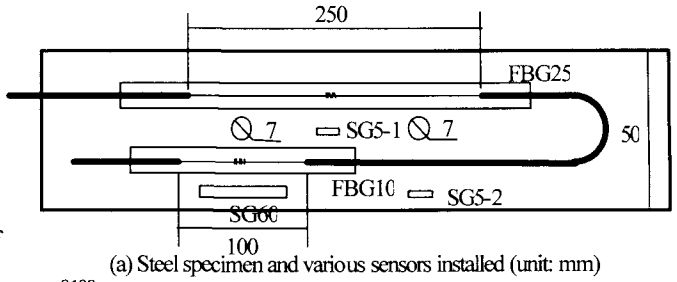

(a) Steel specimen and various sensors installed (unit: mm)

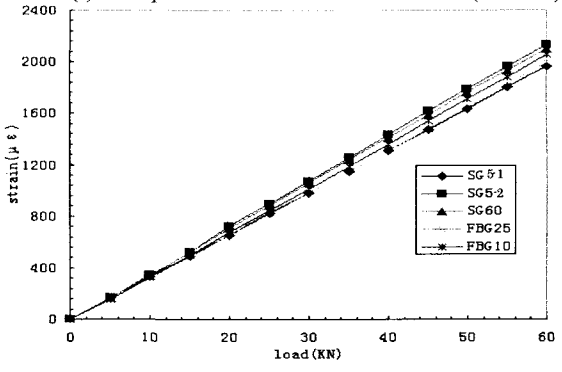

(b) Tensile strains from different sensors

Fig.3. Strain measurements of damaged steel specimen under uniaxial tension

50mm×3mm and two holes of 7mm diameter was designed. Three strain gauges (SG5-1, SG5-2, SG60) and two packaged FBG sensors (FBG10, FBG25 with gauge length of 100mm, 250mm) were adhered onto the specimen surface. Theoretically, relative to the strains from SG5-1, the ratios of strains from SG5-2, SG60, FBG10, FBG25 are 1.145, 1.015, 1.009, 1.007, respectively. Fig.3(b) show the same variation trend as well.

3.2. Concrete specimen under uniaxial compression

In uniaxial compression test, a concrete cylinder with 150mm diameter and 300mm height was loaded with a loading rate of 0.1N/mm^2/sec. up to the failure of the specimen. A packaged FBG sensor and two strain gauges were attached onto the concrete surface, denoted as FBG60, SG60 and SG5 (see Fig.4(a)), whose gauge length is 60mm, 60mm and 5mm respectively. The compressive strains from different sensors versus time are shown in Fig.4(b). It can be found that the strains obtained by FBG60 and SG60 match well but present the obvious difference, especially after initial stages of loading, from those obtained by SG5 which acted as a point sensor. In other words, the packaged long-gage FBG sensor shows the ability for average strain measurements under compression and persistent efficiency even when the maximum compressive strains amount to 1500$\mu\varepsilon$. It should be also noted from the magnified part in Fig.4(b) abrupt variances of strains from FBG sensor occur in some special time, which bring on the shift of time-strain curve of FBG60 from that of SG60 and can be

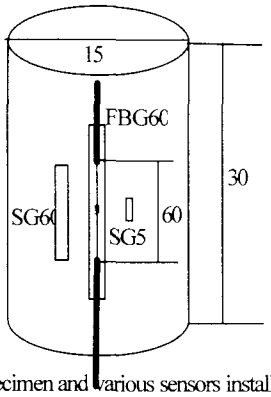

(a) Concrete specimen and various sensors installed (unit: mm)

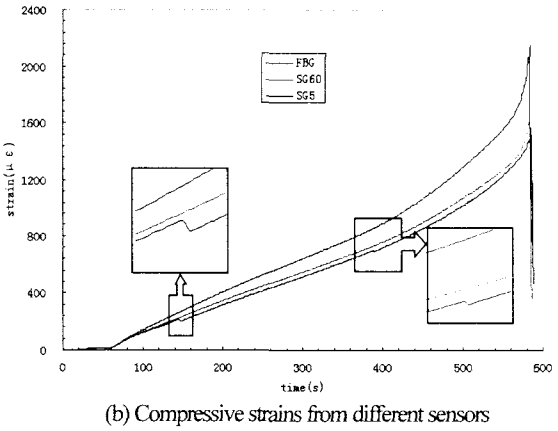

(b) Compressive strains from different sensors

Fig.4. Strains of concrete specimen under uniaxial compression

explained by the possible reason that micro-crack, as appeared at the critical location shown in Fig2, weakened the bonding between concrete and FBG sensor.

3.3. Copper beam under bending

According to bending theory, for a beam under bending with a fixed FBG sensor of gauge length L, distance y away from inertia axis, the static macro-strain measurements can be obtained as:

$$\bar{\varepsilon}_{GL} = \frac{\Delta L}{L} = \frac{\int_0^L \varepsilon(x)dx}{L} = \frac{\int_0^L \frac{y}{\rho(x)}dx}{L} = \frac{y}{L}(\theta(L)-\theta(0)) \quad (1)$$

ρ is the bending curvature, θ is the rotation

Here, a copper beam with 1m length, 27mm width and 5mm height was taken as a specimen for bending tests. Compared with theoretical values shown in Eq.(1), the applicability of FBG sensor for measuring the macro-strain of flexural beams is discussed as follows.

(1) Test setup

A series of beam tests with different boundary condition and mass distribution for 8 testing cases are shown in Table 2.Three types of packaged FBG sensors (called FBG1, FBG10, FBG20 with gauge length of 10mm, 100mm, 200mm) and four strain gauges (called SG1, SG2a SG2b, SG3) were surface-bonded onto the specimens (see Fig.5). To compare the strain values measured in different cases, the average strain from SG2a and SG2b was set to unity, and other strains were determined relative to this reference value. Therefore, a ratio, namely strain ratio, denoted as $\xi_\varepsilon = \varepsilon / \varepsilon_{SG2}$ is introduced. Here, c1 is in the unloaded situation and taken as a reference case..

Table 2. Eight cases of bending test

beam	m (kg)	case
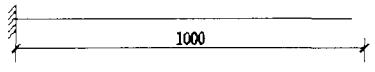	0.0	c1
	0.5	c2
	1.0	c3
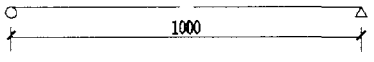	0.5	c4
	1.0	c5
	2.0	c6
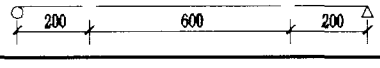	0.5	c7
	1.0	c8

Table 3. Strain ratios in different cases of bending test

Sensor		FBG1	FBG10	FBG20	SG1	SG3
Theoretical		1.000	1.261	1.345	1.420	0.580
c2	ξ_ε	1.020	1.373	1.371	1.336	0.557
	Error*	2.0	2.1	3.4	5.9	4.0
c3	ξ_ε	1.018	1.352	1.367	1.333	0.553
	Error*	1.8	0.5	3.7	5.7	4.7
Theoretical		1.000	0.707	0.605	0.514	0.495
c4	ξ_ε	1.047	0.645	0.485	0.739	0.495
	Error*	4.7	6.6	5.7	4.5	0.0
c5	ξ_ε	1.022	0.619	0.474	0.730	0.483
	Error*	2.2	2.3	7.8	3.2	2.3
c6	ξ_ε	1.012	0.640	0.507	0.751	0.505
	Error*	1.2	5.9	1.3	6.3	2.0
Theoretical		1.000	1.000	1.000	1.000	1.000
c7	ξ_ε	1.075	1.022	0.923	1.086	0.934
	Error*	7.5	2.2	7.7	8.6	6.6
c8	ξ_ε	1.038	1.061	0.939	1.074	0.972
	Error*	3.8	6.1	6.1	7.4	2.8

* Relative errors of measured strain ratios to the oretical value (%)

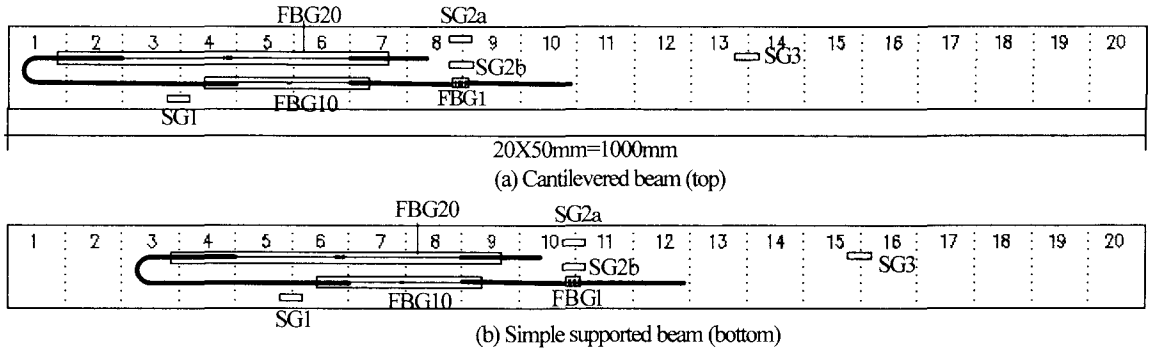

Fig.5. Beams for bending tests and sensor placements

(2) Experimental results

Table 3 shows the strain ratios from different sensors in the eight cases of above bending test. Each of the relative error between measured and theoretical values is calculated as well. It can be found that the errors from FBG sensors vary in a similar range as that from strain gauges. The difference from numerical results may be caused by boundary condition, material properties and noise from experimental environment.

4. Parameters estimation of beams based on static macro-strain measurements

Based on the concept of system identification (SI) algorithms originally developed by Sanayei [9,11], an optimization-based parameter estimation method is presented to adjust the parameters of a finite element model with static macro-strain measurements. Without loss of generality, an Euler-Bernoulli beam is considered here. Forces are applied at a series of Degrees of Freedom (DOFs) and a limited number of macro-strains can be measured at a subset of structural components. The Taylor series expansion of the macro-strain error estimator is utilized to form a sensitivity matrix. A parameter grouping technique is also used to reduce the number of system parameters to satisfy a prescribed identifiability criterion. By means of Gauss-Newton method, an iterative approach is established to update structural model and estimate structural parameters. Instead of elaborated discussion which is available in the above two literatures, some different details are introduced as follows.

4.1. Macro-strain versus displacement relation of beam element and basic model equation

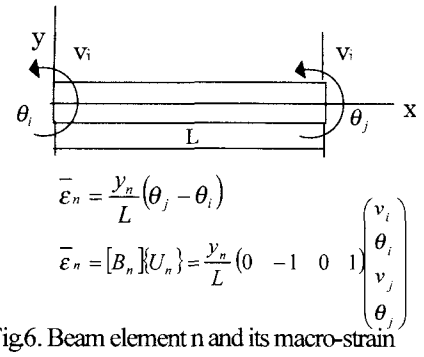

Fig.6. Beam element n and its macro-strain

Fig.6 shows a beam element with two local DOFs at each node, one for vertical translation v and the other for rotation θ. As discussed in Fig.5, the macro strain of this element has a clear relation with rotational degree at two nodes, which can be arranged into matrix form as well. In the same way, the average strain of several consecutive elements can be obtained from the rotational degree at first node of first element and second node of last element on the assumption that y_n and L of each element are same. Actually, this assumption is reasonable for the practical application of sensors and can be easily satisfied by use of suitable finite-element model. That is, once finite-element model of a beam and the location of long-gage sensors are fixed, the mapping vector [B] of size *NSE*×*NDOF* can be formulated, where *NSE*, *NDOF* represent the number of sensors and DOFs. So the mathematical model of a beam based on static macro-strain measurements can be represented by the following equilibrium equation:

$$\{\bar{\varepsilon}\} = [B][K(p)]^{-1}\{F\} \tag{2}$$

where $\{\bar{\varepsilon}\}$ = *NSE* × *NLD*; $[K(p)]$ =*NDOF* × *NDOF*; $\{F\}$=*NDOF*×*NLD*. Here, *NLD* is the number of load cases.

4.2. Macro-strain error function and sensitivity matrix

To evaluate the discrepancy between the analytical and measured macro-strains, an error function, called as "macro-strain error function" is defined as:

$$[e(P)] = \{\bar{\varepsilon}(P)\}^a - \{\bar{\varepsilon}\}^m = [B][K(P)]^{-1}[F] - \{\bar{\varepsilon}\}^m \tag{3}$$

The superscript a is used for analytical values and m for measured values. [B], as mentioned above, is the mapping vector between macro-strain and displacement. [K(P)] is the structural stiffness matrix denoted by unknown parameter vectors $\{p\}$ of size NPA×1 . The error function is of size NSE×NLD, which can be vectorized by reconstructing all the columns vertically into $\{e(p)\}$ of size NM(=NSE×NLD)×1. A first-order Taylor series expansion is used to linearize the vector as:

$$\{E(p+\Delta p)\} \cong \{E(p)\} + [s(p)]\cdot\{\Delta p\} \tag{4}$$

where $[s(p)] = \left[\frac{\partial\{E(p)\}}{\partial\{p\}}\right]$, which is a sensitivity matrix mathematically called Jacobi matrix of size NM×NPA. The jth column of $[s(p)]$ is as follows:

$$\{s_j(p)\} = -[B][K(p)]^{-1}\frac{\partial[K(p)]}{\partial p_j}[K(p)]^{-1}\{F\} \tag{5}$$

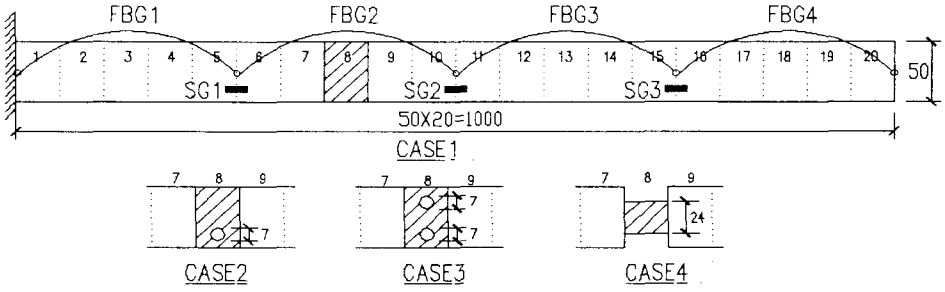

Fig. 7. Four cases including intact and damaged beams

Table 4. Static stain in different cases ($\mu\varepsilon$)

sensor	FBG1	FBG2	FBG3	FBG4	SG1	SG2	SG3
theoretical	600	429	258	86	515	343	172
case1	592	452	257	83	515	340	170
case2	583	453	258	84	515	325	165
case3	586	463	260	81	520	335	170
case4	581	547	268	81	520	335	170

4.3.Target function and iterative procedure for optimization

By taking the Euclidean norm of the error vector, a scalar performance error function, $J(P) = [e(P)]^T [e(P)]$ is adopted as target function for optimization. So the problem turns to find optimum $\{p\}$ to make J (P) minimal. That is, $\frac{\partial J(p)}{\partial \{p\}} = \{0\}$. So the following relationship can be derived:

$$[s(p)]^T [E(p) + [s(p)]\{\Delta p\}] = \{0\} \tag{6}$$

This equation leads to three kinds of solution for $\{\Delta p\}$ due to the number of independent measurements (NM) and unknown parameters to be identified (NPA):

If NM=NPA, $[s(p)]$ is square, so $\{\Delta p\} = -[s]^{-1}\{e(p)\}$

If NM>NPA, the least-squares method results in:

$$\{\Delta p\} = -\left([s]^T [s]\right)^{-1} [s]^T \{e(p)\} \tag{7}$$

If NM<NPA, the physically meaningful solution can not be obtained. Some regulation methods such as parameters grouping should be considered.

4.4. Parameter grouping technique

For large-scale structures, the number of independent system parameters becomes very huge if each member is assigned a certain parameter. On the other hand, the quantity of measurements cannot always be increased sufficiently due to physical and technical limitations. So some condensation methods and parameter grouping techniques are used to reduce the number of system parameters. Hjelmstad and Shin [12] proposed an adaptive parameter group subdivision algorithm. The basic idea is to separate the damaged parts in FE model by updating the parameter groups sequentially based on the comparison between the estimated and baseline value of a parameter. Nam [13] also presented a binary search scheme in which the separation and merging of parameter groups were repeated until one damaged member is completely separated from the other groups.

In this study, regarding a beam with distributed long-gage sensors, the elements within gauge length of a sensor are arranged to a group and associated with the same set of parameters due to two considerations: first, long-gage sensors are used to obtain average strain which unify the measurements within gauge length; second, in the static case strains from a sensor are only sensitive to the parameters at the local length where the long-gage sensor is installed.

5. Experimental verification for a beam installed with distributed long-gage FBG sensors

5.1. Experimental set up and static measurements

A steel cantilevered beam with 1m length, 50mm width and 3mm height was taken as an object structure for parameter identification. Four cases including intact beam and beams with different damage are shown in Fig.8. Four FBG sensors of 250mm gauge length are fixed as a kind of distributed sensor. Three strain gauges are used for comparison. The static measurements from these sensors in one loading case are shown in Table 4. It can be found that the measurements from strain gauges vary little and in some sense show the weakness of conventional point sensors for damage detection in that local strains are not sensitive to structural damage unless the sensors are placed in the vicinity of damage which is obviously impractical. In contrast, although the strains from FBG1, FBG3 and FBG4 change little, those from FBG2 increase with the occurrence and development of damage. The application of distributed long-gage FBG sensors to identify structural parameter will be discussed as follows combined with the SI algorithm mentioned above.

5.2. Damage Identification of beam using static macro-strain measurements from FBG sensors

The flexural stiffness EI of beam elements with known exact value 21.34 is taken as object parameters for identification. All the elements within the gauge length of the FBG sensors (e.g. element 1~6) are arranged to a group and share the same flexural stiffness (denoted as EI1~EI4 for FBG1~FBG4) in common. Based on the above-mentioned SI algorithm, identified parameters in different cases are shown in Fig.8. With reference to the identified parameter of baseline structure using

the measurements from case1, the damage detection results can be seen in Fig.9. The agreement between exact value and analytical value using theoretical strains shows the high accuracy of algorithm. It can be seen from case4 that distributed macro-strains from FBG sensors present advantage to identify the occurrence, location and extent of damage. However, it should also be noted (see case2 and case3) that average strain, although less susceptible to local stress/strain concentrations, can weaken the sensitivity of measurements to damage, which may be merged by noise in measurements. So

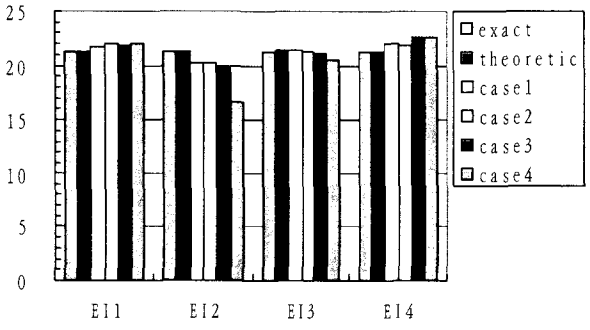

Fig.8. Estimated parameters in different cases

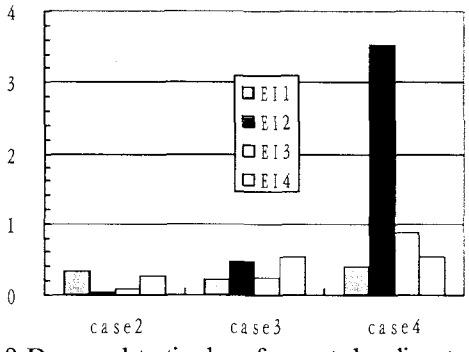

Fig.9. Damage detection by reference to baseline structure

the number of FBG sensors, their respective gauge length and distributed location should be carefully considered for sensor placements.

6. Conclusion

In this paper, a novel packaged long-gage FBG sensor is developed for macro-strain measurements. Static tests show: (1) the static strains of specimens under uniaxial tensile and compressive load can be obtained accurately by FBG sensor and the proposed packaging method has little influence on measurements; (2) the long-gage FBG sensor can measure effectively the average strains of damaged steel and concrete column specimens; (3) the measurements of beam specimen under bending from FBG sensors and corresponding stain gauges show close agreements with theoretical value.

With reference to the concept of SI algorithms originally developed by Sanayei, a static macro-strain based structural parametric identification method is presented. Using the measurements from various sensors, the identified results verify the effectiveness of the presented parametric estimation method and show as well the merits of distributed long-gage FBG sensors over conventional point strain gauge.

References

1) Li H.N., Ren L., Li D.S. and Song G.B., Advances of structural health monitoring by fiber Bragg grating sensor in DUT, *Proceedings of 3rd China-Japan-US Symposium on Structural Health Monitoring and Control*, pp68-79, 2004
2) Ferraro.P and Natale G.D., On the possible use of optical fiber Bragg gratings as strain sensors for geodynamic monitoring, *Optics and Lasers in Engrg.*, pp115-130, 2002
3) W.L.Schulz, J.P.Conte, Eric Udd and M.Kunzler, Real-time damage assessment of civil structures using fiber grating sensors and modal analysis, *Proceedings of SPIE* vol.4696, 2002
4) J.P.Conte, M.Liu and D.Inaudi, Earthquake response monitoring and damage identification of structures using long-gage fiber optic sensors, *Proceedings of Fourteenth Engineering Mechanics Conference*, 2000
5) Branko.G and D.Inaudi, Long-gage fiber optic sensors for global structural monitoring, *First international workshop on structural health monitoring of innovative civil engineering structures, ISIS Canada*, pp285-295,2002
6) D.Inaudi and N.Casanova, Geo-structural monitoring with long-gage interferometric sensors, *Proceedings of SPIE*, 2000
7) M.R.Banan and K.D.Hjelmstad, Parameter estimation of structures from static response. I .Computational aspects, *J. Struct. Engrg., ASCE*, 120(11), pp3243-3258, 1994
8) M.R.Banan and K.D.Hjelmstad, Parameter estimation of structures from static response. II .Numerical Simulation studies, *J. Struct. Engrg., ASCE*, 120(11), pp3259-3283, 1994
9) M.Sanayei and O.Onipede, Damage assessment of structures using static test data, *AIAA Journal*,29(7), pp1174-1179, 1991
10) M.Sanayei , O.Onipede and S.R.Babu, Selection of noisy measurement locations for error reduction in static parameter identification, *AIAA Journal*,30(9), pp2299-2309, 1992
11) M.Sanayei and M.J.Saletnik, Parameter estimation of structures from static strain measurements. I Formulation, *J.Struct.Engrg., ASCE*, 122(5), pp555-562, 1996
12) K.D.Hjelmstad and S.Shin, Damage detection and assessment of structures from static response, *J.Engrg.Mech., ASCE*, 123(6), pp568-576,1997
13) I. Yeo, S.Shin, H.S.Lee, and S.P.Chang, Statistical damage assessment of framed structures from static responses, *J.Engrg.Mech., ASCE*, 126(4), pp414-420, 2000
14) K.Peters, P.Pattis, J.Botsis and P.Giaccari, Experiment verification of response of embedded optical fiber Bragg grating sensors in non-homogeneous strain fields, *Optics and Lasers in Engineering*, 33, pp107-119, 2000
15) K.Lau, L.Yuan and L.zhou, Thermal effects on an embedded grating sensor in an FRP structure, *Smart Materials and Structures*, 10, pp705-712, 2001
16) Mallick P K 1997 *Composite Engineering handbook* (New York: Dekker)

(Received: April 15, 2005)